Ceramics International 30 (2004) 1707–1710

CERAMICS INTERNATIONAL

www.elsevier.com/locate/ceramint

Brillouin scattering investigations of lead magnesium niobate–lead titanate single crystal

G. Shabbir*, S. Kojima

Institute of Materials Science, University of Tsukuba, Tsukuba, Ibaraki 305-8573, Japan

Received 28 November 2003; received in revised form 20 December 2003; accepted 23 December 2003

Available online 6 May 2004

Abstract

Lead magnesium niobate–lead titanate (PMN–PT) [0 0 1] single crystal of morphotropic phase boundary (MPB) composition; have been studied by 90A Brillouin scattering technique. Two phase transition anomalies were observed in the temperature dependences of Brillouin frequency shift (ν) and full-width at half-maximum of the LA and TA modes at $T \sim 336$ and $\sim$415 K associated with symmetry changes from $R3m$ to $P4mm$ and $P4mm$ to $Pm\bar{3}m$, respectively. The observed spectra showed strong polarization dependence in cubic and tetragonal phases, whereas in rhombohedral phase both the VV- and VH-scattering spectra were similar. This effect was attributed to the rotation of spontaneous polarization due to change of symmetry from $P4mm$ to $R3m$.

Keywords: Ferroelectrics; Relaxor; PMN–PT; Morphotropic phase boundary; Brillouin scattering

1. Introduction

The relaxor based $Pb(Zn_{1/3}Nb_{2/3})O_3$–$PbTiO_3$ (PZN–PT) and $Pb(Mg_{1/3}Nb_{2/3})O_3$–$PbTiO_3$ (PMN–PT) complex perovskite type ferroelectric single crystal systems compared to modified $Pb(Zr_xTi_{1-x})O_3$ (PZT) ceramics, show excellent electromechanical properties at room temperature when poled along [0 0 1] cubic direction [1–3]. The electromechanical coupling factor k_{33} is about 0.94 for PMN–33%PT single crystal. The piezoelectric coefficient d_{33} is about 2820 pC/N and 2900 pC/N for PMN–33%PT, and PZN–8%PT, respectively [1,4]. These compositions belong to the morphotropic phase boundary (MPB) regions in PMN–PT and PZN–PT systems. The compositions near the MPB possess extremely attractive applications in making large displacement actuators, high sensitivity medical ultrasonic imaging transducers with superior broadband characteristics, and many other devices like ferroelectric nonvolatile random access memories (NVRAMs) and in high bit density metal–oxide-semiconductor (MOS) dynamic random access memories (DRAMs).

The PMN–PT system is advantageous over the other solid solution systems, such as PZN–PT and $Pb(Sc_{1/2}Nb_{1/2})O_3$–$PbTiO_3$ (PSN–PT) due to its high stability of the perovskite structure and the excellent piezo/ferroelectric properties. In PMN–PT single crystals, the MPB compositions have a molar content of PT close to 0.33. From the structural point of view, the MPB has been believed to be an almost vertical boundary that separates the tetragonal ($P4mm$) and rhombohedral ($R3m$) phases in these systems. Recent structural studies by synchrotron X-ray powder diffraction [5] revealed a monoclinic (Cm) phase with a narrow composition range lying between the rhombohedral and tetragonal phases. In PMN–PT, the width of monoclinic phase was estimated to be $\Delta x \approx 0.03$ with crystal symmetry Pm. Since the intermediate monoclinic phase has been found in the range of MPB in many piezoelectric materials, a natural presumption is that the extraordinary piezoelectric properties are related to the monoclinic phase. However, piezoelectric response in the monoclinic phase was not as strong as that observed in the crystals containing the rhombohedral phase with a composition near the MPB [6]. The anomalous enhancement of piezoelectric constants near MPB has been associated to the 90° domain rotation [7]. However, quenched random fields have been suggested [8] as facilitators for the formation of metastable ferroelectric monoclinic and orthorhom-

* Corresponding author. Tel.: +81-29-853-5262; fax: +81-29-853-5262.
E-mail address: shabbir@ims.tsukuba.ac.jp (G. Shabbir).

0272-8842/$30.00 © 2004 Elsevier Ltd and Techna Group S.r.l. All rights reserved.
doi:10.1016/j.ceramint.2003.12.148

bic phases.

In spite of extensive investigations on MPB compositions, the physical mechanism responsible for the excellent performance of these materials is still unclear. In continuation of our previous results [9] we present here extended Brillouin scattering data on PMN–PT MPB single crystals in wider temperature range and measuring polarization dependence.

2. Experimental procedure

PMN–PT MPB [0 0 1] crystals were grown by Bridgman method. Sample of an approximate size of 10 mm × 10 mm × 2 mm was polished to optical quality and used for present measurements. Inelastically scattered light, excited by a single mode Ar^+-ion laser with a wavelength of 514.5 nm and at a power of ∼100 mW, was analyzed by using a 3 + 3 pass tandem Fabry–Perot interferometer (FPI) and detected by a photomultiplier tube followed by a conventional photon-counting system to detect and average the signals. An additional microscope was fixed at the entrance pinhole of the FPI for precise focusing of the scattered light into the FPI. The laser output power used was appropriate to obtain a reasonable signal and minimize possible local heating. The spectra were recorded from room temperature to ∼500 K. The sample was fixed in a ceramic sample holder and placed inside a home-made tube-furnace specially designed for optical experiments. Temperature was monitored with a CHINO KP-1000 digital temperature controller and the measurements were accurate within ±5 K. An unconventional Brillouin scattering geometry 90A [10], was employed in these measurements. In this scattering geometry the sample is placed symmetrically such that the direct and scattered light emerges at the same angle θ in air. By simple application of the law of refraction the Brillouin shift is obtained for a constant scattering vector of magnitude

$$|q| = \frac{4\pi}{\lambda_i}\sin\theta$$

where λ_i is the wavelength of the incident light in vacuum. The scattering angle θ was adjusted approximately to 90° resulting a scattering vector of a magnitude of $\sim 1.73 \times 10^5\ \mathrm{cm}^{-1}$. The 90A-scattering geometry is more appropriate to study the acoustic properties than the back-scattering one because the acoustic wave vector does not depend on the refractive index of the sample. Moreover; in this kind of geometry bulk phonon modes are probed rather than any kind of surface states (Fig. 1).

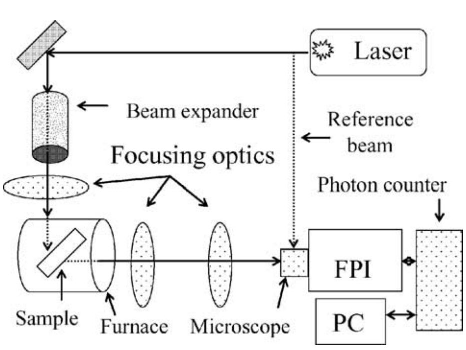

Fig. 1. Block diagram of the 90A Brillouin scattering geometry.

Dielectric permittivity of the crystal was also measured by using a Solartron Impedance analyzer (SI1260). Measurements were done at a heating rate of 1 K/min and 1 V probing ac-signal.

3. Results and discussion

The typical Brillouin spectra associated with the acoustic phonon modes propagating along [1 0 0] directions at different temperatures are shown in Fig. 2. These spectra are composed of one LA mode and one TA mode. In addition, a quasielastic central peak (CP) can be seen clearly in the spectra shown. These spectra were taken in heating the crystal from room temperature to ∼473 K. By assuming the instrumental function as Gaussian, LA, and TA phonon peaks were fitted with the Lorentzian function to obtain ν and phonon damping. The resulting temperature dependences of ν and phonon damping are shown in Figs. 3 and 4, respectively.

The polarization dependent spectra measured in VV- and VH-scattering geometries are shown in Fig. 5. Below $T \sim 420$ K, precision analysis of Brillouin shift ν of the TA Brillouin component was made difficult by the overlap of a strong central peak. The dielectric anomaly at ∼423 K (Fig. 6) shows a typical paraelectric to ferroelectric phase transition character where the symmetry changes from cubic ($Pm\bar{3}m$) to tetragonal ($P4mm$).

The Brillouin scattering results show clearly two discontinuities in $\Delta\nu/\Delta T$ and damping (Figs. 3 and 4) at $T_{\mathrm{T-R}} \sim 336$ K and $T_{\mathrm{C-T}} \sim 415$ K, respectively, with increasing tem-

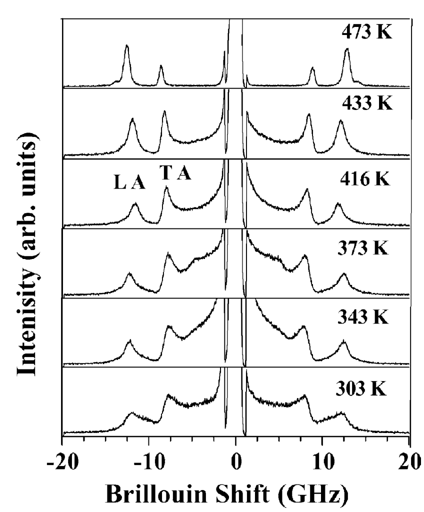

Fig. 2. Typical Brillouin spectra of a PMN–PT MPB single crystal measured at some selected temperatures.

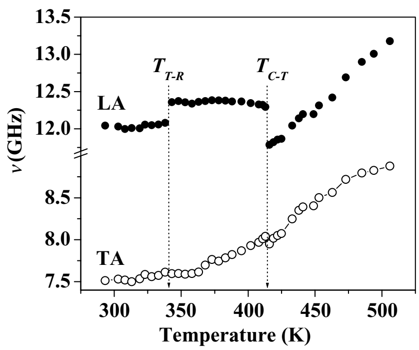

Fig. 3. Temperature dependence of the Brillouin frequency shift (ν) of the LA (filled circles) and TA (open circles) modes of a PMN–PT MPB single crystal.

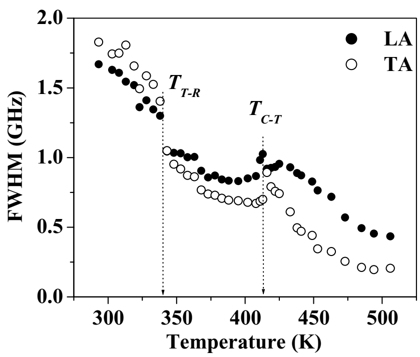

Fig. 4. Temperature dependence of the FWHM of the LA (filled circles) and TA (open circles) modes of a PMN–PT MPB single crystal.

perature. $T_{\mathrm{C-T}}$ is consistent with results of Li et al. [11] while $T_{\mathrm{T-R}}$ has lower value. The optical investigations of the domain configuration of PMN–35%PT single crystal [12] revealed that rhombohedral and tetragonal phases may coex-

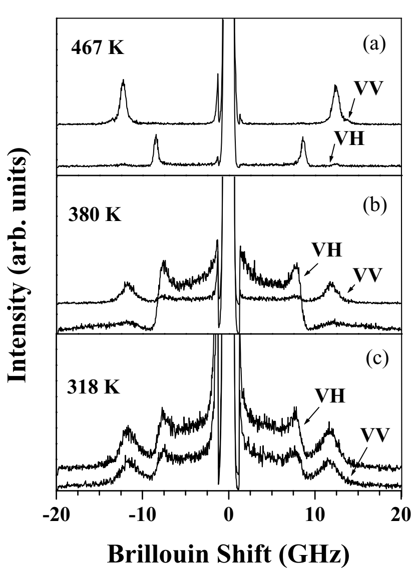

Fig. 5. Observed Brillouin spectra in VV- and VH-scattering geometries in: (a) cubic, (b) tetragonal, and (c) rhombohedral phases, respectively.

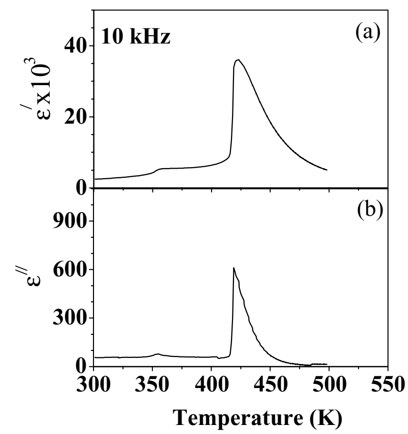

Fig. 6. Real (a) and imaginary (b) parts of the dielectric permittivity of a PMN–PT single crystal as a function of temperature measured at 10 kHz.

ist at room temperature, with transition from $R3m$ to $P4mm$ phase taking place over a wide temperature interval. Moreover, due to compositional fluctuations (even small), a rather wide range of $T_{\mathrm{T-R}}$ exists, instead of a single well defined transition temperature.

The two anomalies in $\Delta\nu/\Delta T$ curve of the TA mode are not clear, however. The smearing out of these discontinuities might be due to existence of a strong coupling mechanism between the TA mode and CP (Figs. 2 and 5) below $T_{\mathrm{C-T}}$. In the rhombohedral and tetragonal phases, $\Delta\nu/\Delta T$ of LA mode remains almost constant within the experimental error although being different by a magnitude of ~2.3%. This small change could not be observed in the Brillouin measurements on PMN–35%PT by Jiang and Kojima [13] probably due to use of larger FSR (~100 GHz). At $T_{\mathrm{C-T}}$, relatively a larger change in ν (~−4.3%) was observed and an increasing trend with further rise in temperature. The sharp damping anomaly at ~415 K exhibited by both modes is usually attributed to a rapid growth of long-range ferroelectric ordering [14].

From the VV- and VH-polarized spectra (Fig. 5) one can see that Brillouin selection rules are valid in cubic (Fig. 5a) and tetragonal (Fig. 5b) phases, whereas below $T_{\mathrm{T-R}}$, both the polarized and de-polarized spectra are similar. The spectra of Fig. 5c indicates that the polar axis has been changed from [0 0 1] ($P4mm$) to pseudocubic [1 1 1] ($R3m$) or any where between [0 0 1] and [1 1 1] (monoclinic m). But the monoclinic phase (M_{A}) appears in PMN–35%PT crystal at room temperature only by poling the crystal under high-field along the [0 0 1] cubic direction. Whereas, unpoled or weekly poled crystal shows an average rhombohedral symmetry [5]. Optical investigations showed that for unpoled PMN–33%PT crystals, the monoclinic phase with various angles of polarization rotation coexists with the rhombohedral phase at room temperature [15]. Present measurements were done above room temperature, therefore, it would be appropriate to argue that the low temperature phase is rhombohedral and not monoclinic one. This can be confirmed by the angle dependence measurements of the Brillouin spectra which is planned to be carried in future.

A strong CP was also observed in present measurements. In PMN, CP has been investigated by Raman scattering [16] caused apparently by the displacement of off-center ions. In case of PMN–PT MPB the coexistence of tetragonal and rhombohedral symmetries complicates to explain such phenomena quantitatively. Most probably the atomic disorder created by the A- and B-site atomic shifts, displacement of Pb ions, and presence of stoichiometric nonuniformities and defects may be responsible for the CP.

Dielectric data plots (Fig. 6) represent a typical ferroelectric behavior dominated by the long-range ferroelectric ordering. The imaginary part (ε''), known as dielectric absorption, was calculated from the product of the dielectric constant and the loss factor. Two transition peaks, paraelectric-cubic to ferroelectric-tetragonal and ferroelectric-tetragonal to ferroelectric-rhombohedral/monoclinic are clearly seen. It has been shown that dielectric losses are dominated by structural irregularities in PMN–PT crystals due to compositional fluctuations (even small) [17].

4. Conclusion

Phase transition anomalies have been studied in PMN–PT MPB [0 0 1] single crystal by the Brillouin scattering technique in 90A-scattering geometry. The LA and TA phonon modes showed two transition anomalies at ∼336 and ∼415 K, corresponding to rhombohedral-tetragonal and tetragonal-cubic phase transition temperatures, respectively. The observed spectra showed strong polarization dependence in VV- and VH-scattering geometries. TA phonon mode and CP showed the strong mode coupling in tetragonal and rhombohedral phases.

Acknowledgements

Financial support for this work was provided by the 21 Century COE program under the Japanese Ministry of Education, Culture, Sports, Science and Technology. One of the authors (G.S.) is thankful to the D.G. PINSTECH, Islamabad, Pakistan for grant of study leave, and to the Japanese Government for a Monbusho scholarship.

References

[1] S.E. Park, T.R. Shrout, Ultrahigh strain and piezoelectric behavior in relaxor based ferroelectric single crystals, J. Appl. Phys. 82 (4) (1997) 1804.
[2] S.E. Park, T.R. Shrout, Characteristics of relaxor-based piezoelectric single crystals for ultrasonic transducers, IEEE Trans. UFFC 44 (1997) 1140.
[3] S.F. Liu, S.E. Park, T.R. Shrout, L.E. Cross, Electric field dependence of piezoelectric properties for rhombohedral $0.955Pb(Zn_{1/3}Nb_{2/3})O_3$–$0.045PbTiO_3$ single crystal, J. Appl. Phys. 85 (5) (1999) 2810.
[4] R.E. Service, Materials science: shape-changing crystals get shiftier, Science 275 (1997) 1878.
[5] Z.-G. Ye, B. Noheda, M. Dong, D. Cox, G. Shirane, Monoclinic phase in the relaxor-based piezoelectric/ferroelectric $Pb(Mg_{1/3}Nb_{2/3})O_3$–$PbTiO_3$ system, Phys. Rev. B 64 (18) (2001) 184114.
[6] A.A. Bokov, Z.-G. Ye, Ferroelectric properties of $Pb(Mg_{1/3}Nb_{2/3})O_3$–$PbTiO_3$ crystals, Phys. Rev. B 66 (9) (2002) 094112.
[7] T.Y. Koo, S.-W. Cheong, Dielectric and piezoelectric enhancement due to 90° domain rotation in the tetragonal phase of $Pb(Mg_{1/3}Nb_{2/3})O_3$–$PbTiO_3$, Appl. Phys. Lett. 80 (22) (2002) 4205.
[8] X. Zhao, B. Fang, H. Cao, Y. Guo, H. Luo, Dielectric and piezoelectric performance of PMN–PT single crystals with compositions around the MPB: influence of composition, poling field and crystal orientation, Mater. Sci. Eng. B 96 (2002) 254.
[9] G. Shabbir, S. Kojima, Study of acoustic anomalies in $Pb(Mg_{1/3}Nb_{2/3})O_3$–$PbTiO_3$ relaxor single crystal by Brillouin scattering, IUMRS-ICAM, Yokohoma, 2003.
[10] J.M. Vaughan, Brillouin scattering in the nematic and isotropic phases of a liquid crystal, Phys. Lett. A 58 (5) (1976) 325.
[11] D. Li, P. Wang, X. Pan, H. Luo, Z. Yin, Twinning domain in $67Pb(Mg_{1/3}Nb_{2/3})O_3$–$33PbTiO_3$ ferroelectric complex perovskite crystal grown by the Bridgman method, M. Mater. Res. 16 (5) (2001) 1252.
[12] Z.-G. Ye, M. Dong, Morphotropic domain structures and phase transitions in relaxor-based piezo-/ferroelectric $(1-x)Pb(Mg_{1/3}Nb_{2/3})O_3-xPbTiO_3$ single crystals, J. Appl. Phys. 87 (5) (2000) 2312.
[13] F.M. Jiang, S. Kojima, Microhetrogeneity and relaxation in $0.65Pb(Mg_{1/3}Nb_{2/3})O_3$–$0.35PbTiO_3$ relaxor single crystals, Appl. Phys. Lett. 77 (9) (2000) 1271.
[14] M.H. Kouk, S.C. Ng, H.J. Fan, M. Iwata, Y. Ishibashi, Hypersonic frequency softening and relaxation in relaxor ferroelectric $0.8Pb(Zn_{1/3}Nb_{2/3})O_3$–$0.2PbTiO_3$, Solid State Commun. 118 (2001) 169.
[15] G. Xu, H. Luo, H. Xu, Z. Yin, Third ferroelectric phase in PMNT single crystals near the morphotropic phase boundary composition, Phys. Rev. B 64 (2) (2001) 020102.
[16] I.G. Siny, S.G. Lushinikov, R.S. Katiyar, E.A. Rogacheva, Central peak in light scattering by relaxor ferroelectric $PbMn_{1/3}Nb_{2/3}O_3$, Phys. Rev. B 56 (13) (1997) 7962.
[17] S. Priya, D. Viehland, K. Uchino, Importance of structural irregularity on dielectric loss in $(1-x)Pb(Mg_{1/3}Nb_{2/3})O_3-xPbTiO_3$ crystal, Appl. Phys. Lett. 80 (22) (2002) 4217.